

# Dynamic Optimisation of CH<sub>4</sub>/CO<sub>2</sub> Separating Operation using Pressure Swing Adsorption Process with Feed Composition Varies

Seungnam Kim<sup>a</sup>, Daeho Ko<sup>b</sup>, Il Moon<sup>\*,a</sup>

<sup>a</sup>Department of Chemical and Biomolecular Engineering, Yonsei University 262 Seongsanno, Seodaemun-ku, Seoul 120-749, Korea

<sup>b</sup>GS E&C, Gran Seoul 33, Jongro, Jongnogu, Seoul, 110-714, Korea  
 ilmoon@yonsei.ac.kr

Pressure Swing Adsorption (PSA) is widely used process for gas separation. Recently, some researchers have been trying to use this PSA process for upgrading bio-gas. The bio-gas mainly consists of methane and carbon dioxide. Highly purified methane gas can be used for energy production, when the methane gas is separated from the carbon dioxide. However, during bio-gas extraction the composition and flow rate are slowly changing. Due to these changes, undesirable product gas properties of will be obtained. The efficiency of PSA process including recovery, purity and productivity are affected by operating conditions, such as feed pressure, feed velocity, p/f ratio, step-time etc. The aim of this research is dynamic optimization of PSA operation for bio-gas upgrading process considering feed composition variations. The objective is maximization of methane recovery, at the purity constraints, while control variables are step times for each step and Purge/Feed (P/F) ratio at regeneration step.

In this research, robust PSA model is developed for dynamic simulation and optimization using gPROMS™ to solve problem. For improving accuracy of the model, distribution method is used; Central Finite Difference Method (CFDM), 2 level in this model. Especially, the time variables are treated as control variables in this model. Due to the discrete changes of boundary and equations, the solving of this optimization problem needs high skills and strategies. The 'SRQPD' solver, one of the NLP solvers, has been used, applying new equations with binary variables which can describe which time belongs to which step.

## 1. Introduction

High purity methane gas is the one of the most valuable energy source and lately the use of this gas is gradually increasing. Because methane and carbon dioxide bi-mixture can be found in landfill gas, coal bed methane gas and flue gas of several processes, the separation of hydrogen and the carbon dioxide capture from those systems are both promising applications from economic and environmental viewpoint (Agarwal et al, 2009).

In this study, the Pressure Swing Adsorption (PSA) process is used to separate the methane gas from the methane and carbon dioxide bi-mixture feed gas. Voss (2005) summarized four powerful characteristic of PSA technology: i) improved and established technology, ii) high reliability, iii) flexibility and iv) fully automated operation system. Due to these powerful performances, many researchers have studied the operating and design optimization on PSA process. Ko et al. (2005) optimised performances of CO<sub>2</sub> capture from flue gas using PSA and FVPSA process. They used the Tailored Single Discretization (TSD) method for describing CSS. Hasan et al. (2012) solved design optimisation problems of PVSA based on economic concepts. They used a kriging-based surrogate model to evaluate complex relationships between variables. Nikolic et al. (2009) presented multibed PSA modelling framework. They obtained the relations between number of beds, recovery, purity and productivity.

In this study a 4-step general Skarstrom cycle for separating CH<sub>4</sub> from the CH<sub>4</sub>/CO<sub>2</sub> gas mixture has been used. It includes Pressurization step, Adsorption step, Depressurization step and Regeneration step. The PSA process has discrete steps within its operation. Each step have its step time and the whole appearance of the process is changing by any chance of the length of those step-times. Therefore, this research aimed to optimise the operation strategy which satisfying the changes in condition of feed and the product. Considering only operation conditions as decision variables, the problem of varying feed condition can be solved. The purity of the product effects highly the economic performance, hence the optimisation of this process was performed at 99, 97 and 95 % methane purity constraints. For description of the interactions between two beds, a two-bed train model has been developed and applied cyclic steady state (CSS) concept from Ko et al. (2005) to reduce the computational burden.

## 2. Process Modeling

### 2.1 Two-bed train model

Two-bed train model is described in Figure 1. The general 4-step Skarstrom cycle is applied in this study, which are Pressurization step (PR), Adsorption step (AD), Depressurization step (DP) and Regeneration step (RG). The bed 1 starts with Pressurization step and bed 2 starts with Depressurization step. In Regeneration step, some of the product is using for the catalyst regenerated from other bed. For improving the fidelity of this two-bed train model, the information of purge gas is calculated simultaneously and applied as a boundary condition.

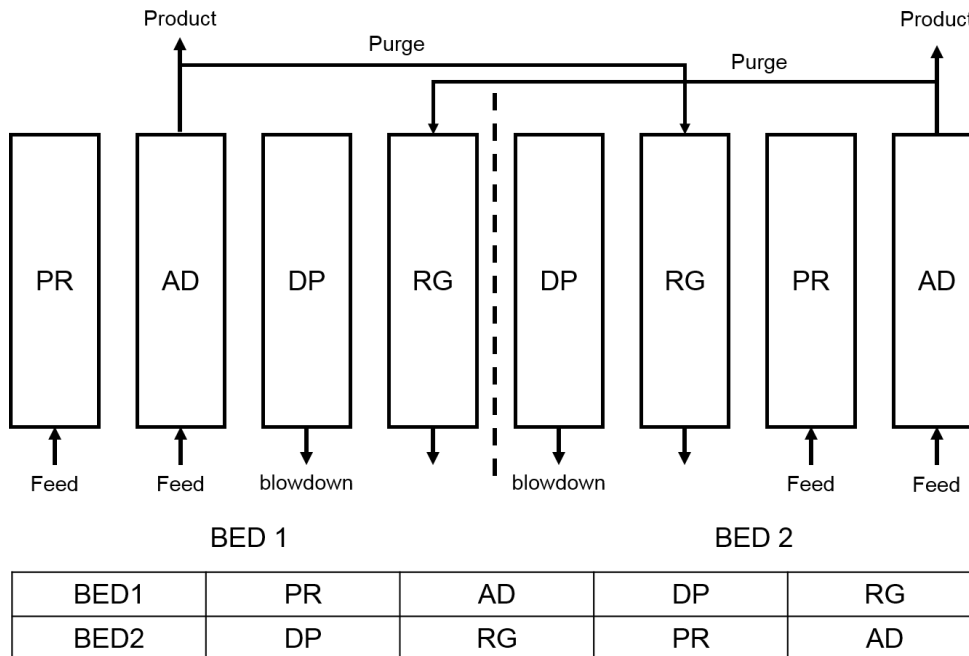


Figure 1: Scheme of the two-bed train PSA process. PR: Pressurization step, AD: Adsorption step, DP: depressurization step, RG: regeneration step

### 2.2 Mathematical modelling

For the mathematical modelling of this system, the following assumptions have been applied.

1. Ideal gas conditions
2. Radial variations is neglected in concentration, pressure and temperature
3. A Linear Driving Force (LDF) model is applied for describing adsorption phenomena.
4. Langmuir-Freundlich (LF) isotherm is applied.
5. The pressure drop in the bed is calculated by Ergun's equation
6. The purge gas has same condition with the product gas of other bed.

The component mass balance equation of the PSA process is the following:

$$\frac{dC_i}{dt} = D_x * \frac{\partial^2 C_i}{\partial z^2} - \frac{\partial u}{\partial z} - \rho_{\text{particle}} * \frac{1 - \epsilon}{\epsilon} * \frac{dq_i}{dt} \quad (1)$$

Where  $C_i$  is the gas concentration of component  $i$ , and  $D_x$  is the axial dispersion coefficient. For describing gas flow in the bed, interstitial velocity,  $u$ , is considered and the  $q_i$  represents solid phase loading for component  $i$ .

Langmuir-Freundlich isotherm is used for adsorption phenomena. The related parameters are adopted from Bae and Lee (2005).

$$q_{eq,i} = q_i^* \frac{bP^{1/n}}{1 + bP^{1/n}} \quad (2)$$

Table 1: Parameters for isotherm adsorption, Bae and Lee (2005)

	T [K]	$q_i^*$ [mmol/g]	b [1/atm]	n [-]	$\Delta q$ [%]
CO <sub>2</sub>	293	5.07 ± 0.23	0.576 ± 0.044	1.90 ± 0.10	3.31
	303	4.86 ± 0.10	0.502 ± 0.015	1.70 ± 0.04	1.45
	313	4.44 ± 0.09	0.456 ± 0.014	1.53 ± 0.04	1.58
CH <sub>4</sub>	293	4.56 ± 0.73	0.232 ± 0.040	1.49 ± 0.17	5.25
	303	4.11 ± 0.41	0.229 ± 0.025	1.45 ± 0.10	3.14
	313	3.73 ± 0.19	0.220 ± 0.012	1.41 ± 0.05	1.58

$q_{eq,i}$  is the adsorbed phase concentration in equilibrium of component  $i$  and  $q_i^*$  means maximum adsorbed phase concentration in equilibrium of component  $i$ .

The mass transfer between two phases is described by linear driving force equation:

$$\frac{dq_i}{dt} = k_i(q_{eq,i} - q_i) \quad (3)$$

Pressure drop inside the bed are captured by Ergun's equation:

$$-\frac{\partial P}{\partial z} = 150 * \mu_{gas} * \varepsilon * \frac{u}{4R_{particle}^2} * \frac{(1 - \varepsilon)^2}{\varepsilon^3} + 1.75 \frac{1 - \varepsilon}{2\varepsilon R_{particle}} u^2 \rho_{gas} \quad (4)$$

And the energy balance in the column is Eq(5) where  $K_l$  is the effective axial thermal conductivity,  $h_{wall}$  is the coefficient for heat transfer between the gas phase and the wall.

$$\begin{aligned} & ((\varepsilon_{bed} + \varepsilon_{particle}(1 - \varepsilon_{bed})) \rho_{gas} C_{pg} + \rho_{bed} C_{ps}) \frac{dT}{dt} + \rho_{gas} * C_{pg} * \varepsilon_{bed} * u * \frac{\partial T}{\partial z} - K_l * \frac{\partial^2 T}{\partial z^2} \\ & - \rho_{bed} * \sum_{i=1}^n (\Delta H_i * \frac{dq_i}{dt}) + 2h_{wall} * (T - T_{wall}) = 0 \end{aligned} \quad (5)$$

Table 2: Boundary conditions

	PR	AD	DP	RG
$z = 0$	$C_i = \frac{y_{feed,i}P}{RT}$	$C_i = \frac{y_{feed,i}P}{RT}$	$\frac{\partial C_i}{\partial z} = 0$	$\frac{\partial C_i}{\partial z} = 0$
	$u = \text{valve eq.}$	$u = u_{feed}$	$u = \text{valve eq.}$	$u = \text{valve eq.}$
	$T = T_{feed}$	$T = T_{feed}$	$\frac{\partial T}{\partial z} = 0$	$\frac{\partial T}{\partial z} = 0$
$z = \text{bedlength}$	$\frac{\partial C_i}{\partial z} = 0$	$\frac{\partial C_i}{\partial z} = 0$	$\frac{\partial C_i}{\partial z} = 0$	$C_i = \frac{y_{purge,i}P}{RT}$
	$u = 0$	$u = \text{valve eq.}$	$u = 0$	$u = -u_{purge}$
	$\frac{\partial T}{\partial z} = 0$	$\frac{\partial T}{\partial z} = 0$	$\frac{\partial T}{\partial z} = 0$	$T = T_{feed}$

### 3. Optimisation

#### 3.1 Cyclic Steady State CSS

Usually, tens of cycles are needed at least for reaching the cyclic steady state. However, this leads to heavy computational burden. To reduce computational time, Ko et al. (2005) retrofitted a new approach on their model. They described the CSS with a new variable,  $\epsilon$ , and defined the following Eq(6).

$$-\epsilon \leq \phi(z_i, 0) - \phi(z_i, t_{cycle}) \leq \epsilon, \quad i = 1, \dots, n \quad (6)$$

The  $\epsilon$  is set to  $10^{-10}$  and thereby, the absolute value of differences between initial and final condition are smaller than  $10^{-10}$ . These variables are treated as inequality end point constraints in optimisation model and all the calculated values are located between  $-10^{-10}$  and  $10^{-1}$ .

### 3.2. Objective, control variable and constraints

The objective of this optimisation model is:

$$\min z = -\text{recovery}_{\text{CH}_4} + 10^7 * \epsilon \quad (7)$$

The  $\epsilon$  is the small positive coefficient for the CSS and the  $\text{recovery}_{\text{CH}_4}$  is the molar recovery of methane. Eq(7) stands for the maximizing methane recovery and for the minimizing differences between initial and final values for satisfying cyclic steady state. The purpose of this research is the optimisation of operation conditions where the feed composition varies. Step times for each step and Purge per Feed ratio are the decision variable during this optimisation.

## 4. Optimisation Result

### 4.1. Feed composition variation

The nine cases are defined with different methane molar percent; from 50 to 90 % with 5 % interval. The optimisation results are in Table 3. All cases are optimised on the 99 % methane purity and the 100 Nm<sup>3</sup>/h feed flowrate on Adsorption step. The AD and RG both steptimes are becoming longer when the methane molar fraction in feed increases. The AD steptime increasing leads to high recovery of methane while makes RG steptime longer because the load of catalyst to be rinsed increases. Due to the characteristic of this two-bed train model, the size of AD and RG steptime remains same as well as the PR and DP steptime.

Table 3: Optimisation results on various methane feed compositions

CH <sub>4</sub> feed composition (%)	PR steptime (s)	AD steptime (s)	DP steptime (s)	RG steptime (s)	P/F ratio (%)	CH <sub>4</sub> recovery (%)
50	40	122.889	40	122.889	0.117332	0.681348
55	40	130.680	40	130.680	0.125143	0.691041
60	40	137.980	40	137.980	0.132090	0.701349
65	40	147.710	40	147.710	0.139179	0.711818
70	40	160.046	40	160.046	0.146424	0.722304
75	40	174.374	40	174.374	0.153210	0.733458
80	40	192.355	40	192.355	0.158918	0.747008
85	40	217.618	40	217.618	0.162889	0.763534
90	40	257.630	40	257.630	0.163398	0.783476

### 4.2. Product methane purity variation

Table 4: Optimisation results on various product purity

CH <sub>4</sub> feed composition (%)	Product CH <sub>4</sub> purity (%)	PR steptime (s)	AD steptime (s)	DP steptime (s)	RG steptime (s)	P/F ratio (%)	CH <sub>4</sub> recovery (%)
60	99	40	137.980	40	137.980	0.132090	0.701349
60	97	40	142.274	40	142.274	0.093880	0.764016
60	95	40	144.907	40	144.907	0.074420	0.797809

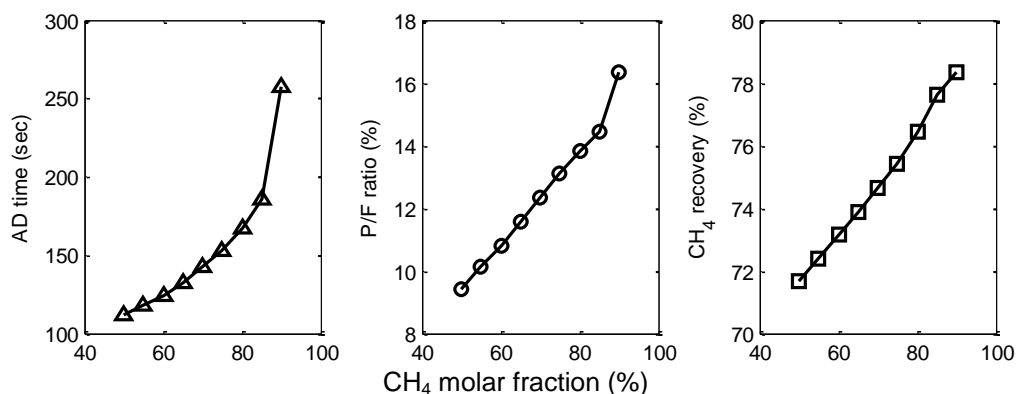


Figure 2: Optimised AD time, P/F ratio and methane recovery result on various methane feed compositions

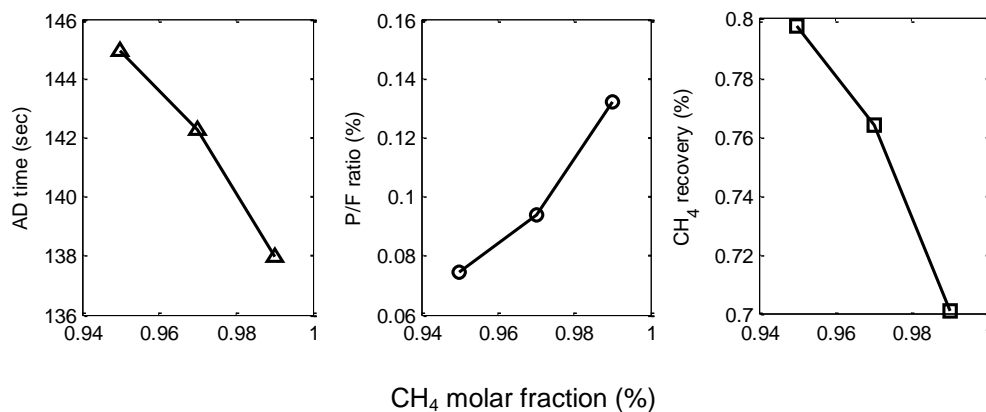


Figure 3: Optimised AD time, P/F ratio and methane recovery result on various product purity

In this chapter, the cases which have different product purity is optimised. The feed methane molar fraction is fixed on 60 % and the product purity conditions are 95, 97 and 99 %. Similarly to chapter 4.1., the decision variables are the operation variables only. With any decrease of the product purity, the AD step time increases slightly and P/F ratio decreases. This PSA optimisation models tends to control P/F ratio than AD step time. In conclusion, decreasing of P/F ratio leads to increasing recovery, and it satisfies target purity through making rinsing efficiency lower.

## 5. Conclusion

This research is focused on optimising operation conditions on various feed compositions without changing process design. The nine cases - from 50% to 90% methane molar fraction- are optimised with step time and P/F ratio as the control variables. The optimisation has been performed for same feed molar fraction cases with different product target purities. According to the results, the differences in P/F ratio were the most effective operating variable and due to the decrease of the P/F ratio, the methane recovery increased as the P/F ratio decrease. All these results show that the operation strategy can lead various product properties without changing design of the process.

## Reference

- Agarwal A., Biegler L., Zitney S., 2009, Simulation and Optimization of Pressure Swing Adsorption Systems Using Reduced-Order Modeling, *Ind. Eng. Chem. Res.*, 48(5), 2327-2343.
- Bae Y.S., Lee C.H., 2005, Sorption kinetics of eight gases on a carbon molecular sieve at elevated pressure, *Carbon*, 43(1), 95-107.
- Dantas T.L., Luna F.M.T., Silva Jr I.J., Torres A.E.B., De Azevedo D., Rodrigues A.E., Moreira R.F., 2011, Carbon dioxide–nitrogen separation through pressure swing adsorption, *Chemical Engineering Journal*, 172(2), 698-704.

- Hasan M., Baliban R., Elia J., Floudas C., 2012, Modeling, Simulation, and Optimization of Postcombustion CO<sub>2</sub> Capture for Variable Feed Concentration and Flow Rate. 2. Pressure Swing Adsorption and Vacuum Swing Adsorption Processes, *Ind. Eng. Chem. Res.*, 51(48), 15665-15682.
- Khajuria H., Pistikopoulos E.N., 2011, Optimization and Control of Pressure Swing Adsorption Processes Under Uncertainty, *AIChE Journal* 59(1), 120-131.
- Ko D., Siriwardane R., Biegler L., 2005, Optimization of pressure swing adsorption and fractionated vacuum pressure swing adsorption processes for CO<sub>2</sub> capture, *Ind. Eng. Chem. Res.*, 44(21), 8084-8094.
- Ko D., Siriwardane R., Biegler L.T., 2003, Optimization of a pressure-swing adsorption process using zeolite 13X for CO<sub>2</sub> sequestration, *Industrial & Engineering Chemistry Research*, 42(2), 339-348.
- Nikolic D., Kikkinides E., Georgiadis M., 2009, Optimization of Multibed Pressure Swing Adsorption Processes, *Ind. Eng. Chem. Res.*, 48(11), 5388-5398.
- Voss C., 2005, Applications of pressure swing adsorption technology, *Adsorption-Journal of the International Adsorption Society*, 11, 527-529.